Spectral evolution of NIR luminescence in a Yb^{3+}-doped photonic crystal fiber prepared by non-chemical vapor deposition

Chao Wang (王 超)[1,4], Guiyao Zhou (周桂耀)[1,2,3,4*], Ying Han (韩 颖)[1,4], Wei Wang (王 伟)[1,4], Changming Xia (夏长明)[2], and Lantian Hou (侯蓝田)[1,3,4]

[1]*College of Information Science and Engineering, Yanshan University, Qinhuangdao 066004, China*

[2]*Laboratory of Nanophotonic Functional Materials and Devices, South China Normal University, Guangzhou 510006, China*

[3]*State Key Laboratory of Metastable Materials Science and Technology, Yanshan University, Qinhuangdao 066004, China*

[4]*Key Laboratory for Special Fiber and Fiber Sensor of Hebei Province, Yanshan University, Qinhuangdao 066004, China*

[*]*Corresponding author: zguiyao@163.com*

Received November 15, 2012; accepted February 25, 2013; posted online May 30, 2013

Silica-based Yb^{3+}-doped glass is prepared by non-chemical vapor deposition. The drawn photonic crystal fiber (PCF) has a strong absorption at 976 nm and emission wavelength of approximately 1 037 nm. The intensity and spectral lineshape of the near infrared (NIR) luminescence of the Yb^{3+}-doped PCF are recorded and discussed in terms of excitation power, excitation wavelength, fiber length, and Yb^{3+} ion concentration. The emission intensifies as the excitation power and Yb^{3+} ion concentration increase. The intensity of the shorter wavelength side of the luminescence spectrum decreases as the length of the PCF increases.

OCIS codes: 160.5690, 160.2290, 060.5295, 060.2400.

doi: 10.3788/COL201311.061601.

Broadly tunable laser sources are readily applied in the studies on spectroscopy, photochemistry, sensing and nonlinear optics, and so on[1]. Double-cladding photonic crystal fibers (PCFs) provide a range of benefits for high-power laser applications, such as extremely high numerical aperture (NA) for inner cladding, which allows efficient pumping with inexpensive/high power pumps. Moreover, the large mode area avoids nonlinearities and provides a good overlap between the pump guide and the signal guide area, which result in high pump absorption and high efficiency[2,3]. Yb^{3+} is a preferred lasing ion because of its long-lifetime excited state and simple energy-level scheme as well as its broad absorption and emission band[4]. Thus, Yb^{3+}-doped PCF lasers are uniquely suitable for continuously tunable lasers. Numerous studies have investigated the optical properties of Yb^{3+}-doped active PCF. Tunable high-power Yb^{3+}-doped double-clad PCF lasers that operate at several defined wavelengths have been demonstrated[5]. A single linearly polarized, widely and freely tunable two-wavelength Yb^{3+}-doped fiber laser has also been reported[6]. Most commercially available high-power rare earth (RE)-doped active laser fibers are produced by modified chemical vapor deposition (MCVD) with solution doping[7,8]. The MCVD with solution doping is very well suited for producing active fiber preforms for single mode fibers with small active core diameters[9]. For high-power fiber lasers and amplifiers, the fibers are required to have large cores, high doping concentrations, and uniform doping. To fabricate these fibers, other preparation routes, such as non-chemical vapor deposition (non-CVD), have been developed. In 2007, Renner-Erny *et al.*[10] prepared a Nd^{3+}-doped fiber utilizing RE oxides and Al_2O_3 oxide, and the fiber exhibited a good laser property. In 2008, Di Labio *et al.*[11,12] prepared multicore RE-doped and single-core fibers with several types of RE using dry RE and Al_2O_3 oxide. Their study showed that the fiber emitted an over-two-octave-spanning fluorescence spectrum. In 2009, Devautour *et al.*[13] proposed a preparation technology of RE-doped glass based on direct sand vitrification, and the laser obtained with the drawn fiber exhibited 74% slope efficiency. In 2011, Leich *et al.*[14] improved the powder sinter technology and obtained a 20-dB/km fiber background attenuation and 80% laser slope efficiency. To the best of our knowledge, studies on spectral evolution of near infrared (NIR) luminescence of Yb^{3+}-doped PCF prepared by non-CVD under different operational conditions that allow well-designed PCF lasers have not been reported.

This letter presents a non-CVD process, a high-temperature melting technology, to prepare Yb^{3+}-doped silica glass. This glass is prepared by stirring and melting to homogenize its structure and components. We observe the spectral evolution of NIR luminescence of drawn Yb^{3+}-doped PCF. Intensity and spectral lineshape variations in the NIR luminescence are recorded and discussed in terms of excitation power, excitation wavelength, PCF length, and Yb^{3+} ion concentration.

Yb^{3+}-doped glass was prepared with the Yb_2O_3–Al_2O_3–SiO_2 composition. Al^{3+} ions prevent RE ions from clustering and increase the solubility of RE ions[15,16]. The purities of Yb_2O_3, Al_2O_3, and SiO_2 were 99.99%, 99.99%, and 99.9999%, respectively. SiO_2 and other components of pure raw material were weighed according to a specific weight proportion. Firstly, the three kinds of powder were mixed in a blender and placed in an oven at 150 °C for 8–10 h to remove moisture. Secondly, the dry powder was sintered into a silica glass by high-

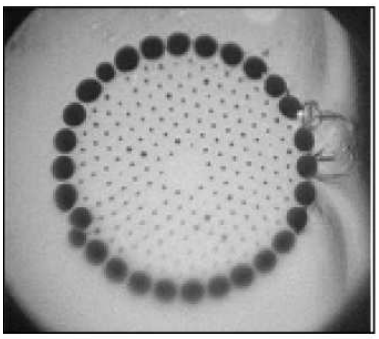

Fig. 1. Cross-section of the Yb^{3+}-doped PCF.

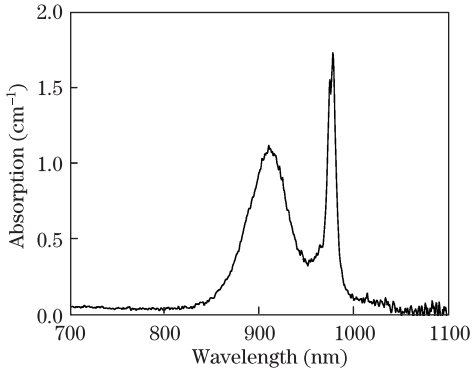

Fig. 2. Absorption spectrum of the Yb^{3+}-doped glass rod.

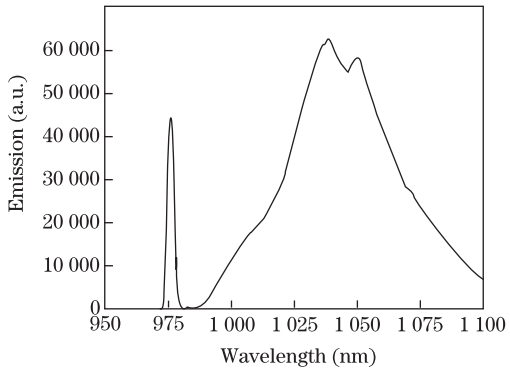

Fig. 3. Emission spectrum of the Yb^{3+}-doped PCF with a length of 0.40 m at the excitation power of 0.20 W.

temperature melting at over 1 950 °C in a pure oxygen atmosphere. The Yb^{3+}-doped glass sample was cut and optically polished into round rods, and the PCF preform was prepared by stack technology. Finally, the preform was drawn into a PCF in a fiber-drawing tower. All the experiment previously mentioned were performed in a super clean environment.

The cross-section of the Yb^{3+}-doped PCF fabricated in our laboratory is shown in Fig. 1.

A halogen lamp was used as a light source of absorption spectrum with a wavelength between 350 and 2 700 nm. The absorption and emission spectrum were recorded by an optical spectrum analyzer (AvaSpec-2048-USB2). All measurements were performed at room temperature (25 ° C). The typical Yb^{3+} absorption in the wavelength region between 800 and 1 100 nm with a broad pedestal, superimposed by a low peak at approximately 910 nm and a narrow high peak at 976 nm, is demonstrated in Fig. 2. The absorption peaks are generated from the ground-state manifold to the different excited-state manifolds of Yb^{3+} ions. The background loss was tested using the cutback method, and the attenuation value of the PCF at 1 200 nm is approximately 0.25 dB/m.

A continuous Ti:Al_2O_3 laser (Mira 900, Coherent, USA) with a tunable laser wavelength from 700 to 980 nm was used as the pump source of the emission spectrum. Figure 3 illustrates the two obvious emission peaks in the emission spectrum of Yb^{3+}-doped PCF, which result from the transition from the different excited-state energy levels to the ground-state energy level of Yb^{3+} ions. The 976-nm peak is due to the unabsorbed pump light. The NIR luminescence spectrum undergoes a remarkable change depending on the PCF length, that is, the interaction length. Figure 4 shows the spectral evolution with three different PCF lengths. The emission peak shifts to a longer wavelength as the PCF length increases, which originates from the radiation trapping because of re-absorption[17,18]. Re-absorption can be explained that the part light emitted by the Yb^{3+} ions in excited states is absorbed again by the Yb^{3+} ions in ground states. As the PCF length increases, the intensity of the shorter wavelength side of the NIR luminescence spectrum becomes smaller than the other side, which leads to a narrower spectral bandwidth. The phenomenological explanation for this behavior is possible because of the dependence of Yb^{3+}-doped PCF re-absorption on wavelength[2] and Rayleigh scattering. Rayleigh scattering is a fundamental loss mechanism arising from density fluctuations frozen into the fused silica during manufacture. Resulting local fluctuations in the refractive index scatter light in all directions. The Rayleigh scattering loss varies as λ^{-4} and is dominant at short wavelengths[19]. Thus, light with different wavelengths will endure different losses and have different gains. However, this spectral variation is difficult to observe when the excitation power, excitation wavelengths, and Yb^{3+} ion concentrations for a fixed length PCF are different. Figures 5, 6, and 7 indicate that the spectral evolution is measured with a fixed PCF length for various excitation powers, excitation wavelength, and Yb^{3+} ion concentration, respectively. The spectral lineshape change with different excitation powers and wavelengths is smaller than that observed in the example of varying PCF lengths. Figure 5

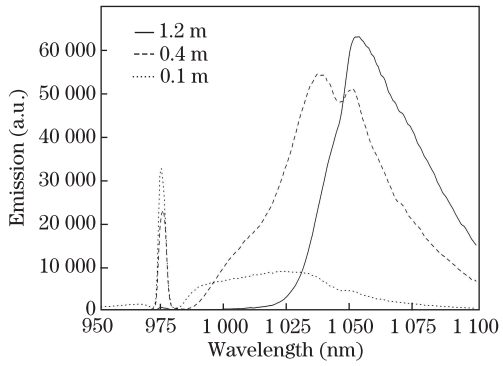

Fig. 4. Emission spectrum of the Yb^{3+}-doped PCF with three different PCF lengths. The excitation power is fixed at 0.15 W at the excitation wavelength of 976 nm for all cases.

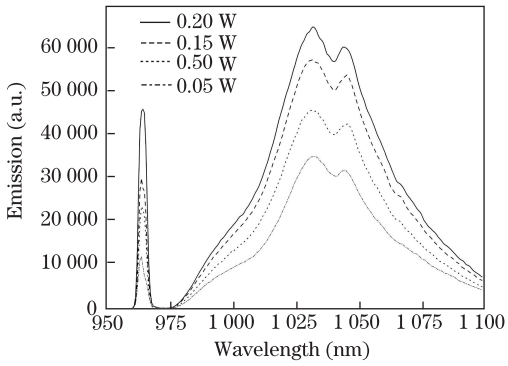

Fig. 5. Emission spectrum of the Yb^{3+}-doped PCF at various excitation powers at the excitation wavelength of 976 nm. The length of the PCF is 0.40 m.

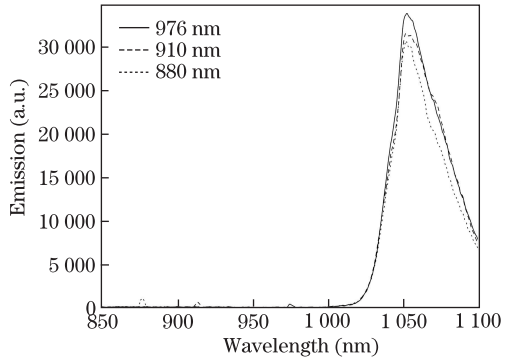

Fig. 6. Emission spectrum of the Yb^{3+}-doped PCF at different excitation wavelengths at the excitation power of 0.10 W. The length of the PCF experiment is 1.20 m.

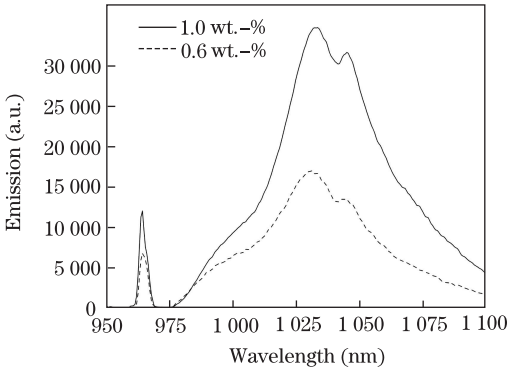

Fig. 7. Emission spectrum of the Yb^{3+}-doped PCF with different Yb_2O_3 concentrations. The excitation power is fixed at 0.05 W with an excitation wavelength of 976 nm. The length of the PCF is 0.40 m.

demonstrates that the NIR luminescence intensifies as the excitation power increases. This result indicates that no power saturation exists when the excitation power is up to 0.20 W.

Although doping concentration can affect the refractive index of the glass, considerable error occurs if this concentration is quantified by the size of the refractive index. Therefore, doping concentration is determined by precisely weighing the proportion of the raw materials (the concentrations of Yb_2O_3 are 0.6 and 1.0 wt.-%), and then the concentration value becomes more accurate. Figure 7 demonstrates that the luminescence intensifies as the Yb^{3+} ion concentration increases when the Yb^{3+} ion doped concentration is below the concentration limit. Otherwise, as the concentration increases, the clustering of Yb^{3+} ion will result in the reduction of the fluorescent lifetime and the laser efficiency of Yb^{3+}-doped active laser PCF[20,21]. The primary luminescence peak shifts to longer wavelength as the Yb^{3+} ion concentration increases, which can be attributed to the alteration of the dominant coordination number of Al^{3+} ion with increasing Yb^{3+}/Al^{3+} ratio. The alteration effectively changes the ill-coordinated state of Yb^{3+} ion to a well-coordinated state because of the increased freedom in the bonding configuration[22].

The broad luminescence spectrum of Yb^{3+} ion allows emitting laser light within a wide range[23]. As shown from the spectral evolution in Figs. 4–7, we can obtain several spectral changes as follows: i) the laser wavelength depends on the PCF length instead of on the excitation wavelength and excitation power; ii) the full width at half maximum (FWHM) of the emission band becomes narrower, i.e., the FWHM decreases from 65 to 42 nm, and the long wavelength has higher gain than the short wavelength as the PCF length increases; iii) the luminescence intensifies when the excitation power and Yb^{3+} ion concentration increase; iv) the expected blue shift is not yet visible in the limited range of available excitation power and different excitation wavelengths. However, increasing Yb^{3+} ion concentration allows the primary emission peak to induce obvious red shift.

In conclusion, we prepare a Yb^{3+}-doped glass by non-CVD. The drawn PCF has good optical properties, which demonstrate typical absorption and emission pattern of Yb^{3+} ions. As the PCF length increases, the emission band shifts to longer wavelength and the spectral bandwidth becomes narrower. The laser wavelength depends on the PCF length instead of on the excitation wavelength and excitation power. The emission intensifies as the excitation power and Yb^{3+} ion concentration increase. The primary emission peak induces evident red shift when the Yb^{3+} ion concentration increases. The non-CVD technology of preparing Yb^{3+}-doped glass and the experimental data provide a basis for further studying and designing a continuously tunable high-power PCF laser.

This work was supported by the State Key Development Program for Basic Research of China (No. 2010CB327604), the State Key Program of National Science of China (No. 60637010), the National Natural Science Foundation of China (No. 61205084), the Natural Science Foundation of Hebei Province (No. F2012203122), the College Science Research Program of Hebei Province (No. Z2010336), and the Jiangsu Meteorological Observation and Information Processing Key Laboratory Open Subject (No. KDXS1107).

References

1. P. Zeil and F. Laurell, Opt. Express **19,** 13940 (2011).
2. H. Su, Y. Li, K. Lu, K. Wang, and Q. Guo, Proc. SPIE **6823,** 682318 (2007).
3. S. J. Liu, H. Y. Li, Y. X. Tang, and L. L. Hu, Chin. Opt.

Lett. **10,** 081601 (2012).

4. J. L. Person, V. Nazabal, R. Balda, J. L. Adam, and J. Fernandez, Opt. Mater. **27,** 1748 (2005).
5. J. K. Sahu, C. C. Renaud, K. Furusawa, R. Selvas, J. A. Alvarez-Chavez, D. J. Richardson, and J. Nilsson, Electron. Lett. **18,** 1116 (2001).
6. D. Liu and C. Wang, Opt. Commun. **283,** 98 (2010).
7. J. Stone and C. A. Burrus, Appl. Phys. Lett. **7,** 388 (1973).
8. J. E. Townsend, S. B. Poole, and D. N. Payne, Electron. Lett. **7,** 329 (1987).
9. A. Langner, G. Schötz, M. Such, T. Kayser, V. Reichel, S. Grimm, J. Kirchhof, V. Krause, and G. Rehmann, Proc. SPIE **6873,** 687311 (2008).
10. R. Renner-Erny, L. Di Labio, and W. Lüthy, Opt. Mater. **29,** 919 (2007)
11. L. Di Labio, W. Lüthy, V. Romano, F. Sandoz, and T. Feurer, Appl. Opt. **47,** 1581 (2008).
12. L. Di Labio, W. Lüthy, V. Romano, F. Sandoz, and T. Feurer, Opt. Lett. **33,** 1050 (2008).
13. M. Devautour, P. Roy, S. Février, C. Pedrido, F. Sandoz, and V. Romano, Appl. Opt. **48,** G139 (2009).
14. M. Leich, F. Just, A. Langner, M. Such, G. Schötz, T. Eschrich, and S. Grimm, Opt. Lett. **36,** 1557 (2011).
15. V. Petit, T. Okazaki, E. H. Sekiya, R. Bacus, K. Saito, and A. J. Ikushima, Opt. Mater. **31,** 300 (2008)
16. V. A. Monteil, S. Chaussedent, G. Alombert-Goget, N. Gaumer, J. Obriot, S. J. L. Ribeiro, Y. Messaddeq, A. Chiasera, and M. Ferrari, J. Non-Cryst. Solids **348,** 44 (2004).
17. G. Toci, Appl. Phys. B **106,** 63 (2012).
18. G. Toci, D. Alderighi, A. Pirri, and M. Vannini, Appl. Phys. B **106,** 73 (2012).
19. G. P. Agrawal, *Nonlinear Fiber Optics* (Academic Press, Waltham, 2007).
20. T. Deschamps, N. Ollier, H. Vezin, and C. Gonnet, J. Chem. Phys. **136,** 014503 (2012).
21. H. Gebavi, S. Taccheo, D. Milanese, A. Monteville, O. Le Goffic, D. Landais, D. Mechin, D. Tregoat, B. Cadier, and T. Robin, Opt. Express **19,** 25077 (2011).
22. K. Arai, H. Namikawa, K. Kumata, T. Honda, Y. Ishii, and T. Handa, J. Appl. Phys. **10,** 3430 (1986).
23. M. Pask, R. J. Carman, D. C. Hanna, A. C. Tropper, C. J. Mackechnie, P. R. Barber, and J. M. Dawes, IEEE J. Sel. Top. Quantum Electron. **1,** 2 (1995).